3D-OSEM Transition Matrix for High Resolution PET Imaging with Modeling of the Gamma-Event Detection

Juan E. Ortuño, George Kontaxakis, *Member, IEEE*, Pedro Guerra, *Student Member, IEEE*, and Andrés Santos, *Senior Member, IEEE*

Abstract –We present an efficient methodology for the calculation of the transition matrix for 3D-OSEM iterative image reconstruction, including a model of the gamma-event detection in crystal with photoelectric and Compton scatter interaction. The method is adapted for high resolution PET cameras composed of pixelated scintillator crystal arrays and with axial symmetry. 2D-OSEM algorithm, in combination with rebinning methods such as SSRB and FORE, can also be performed using a subset of this transition matrix.

I. Introduction

IN PET imaging, iterative image reconstruction (IIR) algorithms can include a detailed statistical model of the high energy gamma ray detection process.

A maximum-likelihood expectation-maximization (MLEM) IIR algorithm follows the next iterative scheme [1]:

$$x_j^{(n+1)} = x_j^{(n)} \left(\sum_{i=1}^{I} a_{ij} \frac{y_i}{\tilde{y}_i^{(n)}} \right) / \left(\sum_{i=1}^{I} a_{ij} \right) \qquad (1)$$

where at each iteration n, the j voxel value is updated, being y_i the acquired projection for the line of response (LOR) i, and:

$$\tilde{y}_i = \sum_{j=1}^{J} a_{ij} x_j \qquad (2)$$

the estimated projection, calculated from the probability a_{ij} that an event generated in the volume of voxel j is detected in LOR i.

Ordered Subset methods [2] group projection data into an ordered sequence of blocks and an ordered subset EM (OSEM) iteration is defined as a single pass through all subsets.

The transition matrix $\mathbf{A} = \{a_{ij}\}$ can be computed analytically by estimating the volume of intersection between the voxel and the volume between the surfaces of the pair of detectors that define the LOR i. In PET cameras it is clear that $a_{ij} = 0$ (no intersection) in the majority of pairs *i-j* and therefore $\mathbf{A}$ is a sparse matrix in a geometric aproximation. These approaches, however, do not consider other physical effects (e.g., depth of interaction, object and crystal scattering, non collinearity, etc.).

Monte Carlo (MC) simulation is an alternative method for the calculation of the transition matrix [3]. This computation can either be based on only the geometrical characteristics of the camera, or can also incorporate models of physical processes related to the gamma-event generation and detection, such as annihilation photon, non collinearity, positron range, inter-crystal penetration, detector and object Compton scatter or object attenuation. Some of these effects, however, are object dependent, and their accurate modeling using Monte Carlo simulation would lead to non-sparse matrices, involving prohibitive reconstruction times and disk storage requirements.

Negligible probability values should be rounded to zero, working with dense data sets, as sparse matrix operations can greatly improve the 3D reconstruction times: in each EM iteration only non-zero values need to be backprojected.

We present here an efficient methodology for the calculation of the transition matrix for 3D-OSEM iterative image reconstruction, including a model of the gamma-event detection in crystal with photoelectric and Compton scatter interaction. The method is adapted to high resolution PET cameras composed of pixelated scintillator crystal arrays and with axial symmetry. 2D-OSEM (possibly in combination with rebinning algorithms [4]) can be also performed using a subset of the transition matrix.

II. Materials and Methods

The proposed technique employs a two-step Monte Carlo (MC) simulation methodology for the generation of the transition matrix. The first MC simulation includes gamma pair generation in the field of view (FOV) and the intersection with the detector. The second MC models the depth of iteration within the scintillator and inter-crystal scatter. The distribution of the energy representing the optical photons generated is discretized and stored in look-up tables (LUT).

A. Generation of gamma pairs and intersection with the detector.

The transition matrix simulator uses voxel-based activity distributions placed in the field of view (FOV). The voxels can be cubic, spherical or cylindrical shaped with optional overlapping. They are located in a uniform cubic grid, although with the object oriented programming technique used, other configurations like polar grids, blobs, etc. can easily be included.

Both positron range and non-collinearity are simulated.

Photon pair non-collinearity is modeled by means of a direction deflection with a Gaussian distribution having a zero-mean and 0.5 degrees FWHM. Deflections greater than a user selected value are discarded, in order to maintain the sparseness of the transition matrix.

The positron range is object and radioisotope dependent. The proposed model approximates fluorine-18 (F18) in water as a sum of two three-dimensional Gaussian distributions [5]. As a result, the activity is smoothed in the voxel edges.

In order to reduce computing, the gamma rays can be generated uniformly solely in directions within the solid angle of coincidences allowed. For tomographs with axial symmetry, only the voxels of the central slice need to be modeled in detail. The values for the rest of the voxels can be calculated based on 2-fold axial symmetries and axial parallel line redundancies [6]

The annihilation photons are followed up to their intersection with the crystal surface. Then, the N crystals with the highest detection probability, according to a previously calculated crystal LUT, are retained generating N^2 weighted lines of response and binned into the corresponding sinogram positions. This method allows to simulate relatively few photons per voxel to obtain statistically significant transition matrix probabilities, instead of tracking individual photons along the crystals which would lead to large simulation times.

B. Crystal LUT simulation.

For incident high energy gamma rays, the detection probability is modeled as a function of the angle of incidence and intersection point. The photon tracking has been modeled using the Klein-Nishina [7] formula and the National Institute of Standard and Technology (NIST) photon cross section tables [8].

The depth of iteration is modelled with the exponential attenuation in crystal $I_x = I_0 e^{-\mu x}$, where the absorption coefficient μ is defined as the total cross section σ, multiplied by the density ρ. The total cross section is the sum of the photoelectric, pair production, coherent and incoherent (Compton) scattering. Only Compton and photoelectric effects are significant for 511 keV gamma rays (Figure 1). Using NIST tables, LSO crystals can be approximated as L_2SiO_5 with a density of 7.4 g/cm^3, and constituents fractions by weight: 17.466% oxygen, 6.132% silicon, and 76.4021% Lutetium. The MC algorithm of Compton and photoelectric crystal interaction has been modeled as follows.

1. Initialize incident direction ϕ_0, position p_0, energy E_0 and absorption coefficient μ_0.
2. Generate a travel distance, $d = -\log(1-\nu)/\mu_i$, with ν being a random number uniformly distributed on $(0,1)$
3. Calculate interaction position $p_{i+1} = f(\phi_i, d_i, p_i)$; if it is located outside the crystal, go to 5.
4. Determine the probability of photoelectric or Compton interaction (photofraction at E_i)
   If photoelectric, sum energy E_i in position p_{i+1}. Go to 4.
   If Compton: sum energy $f(E_i)$ in position p_{i+1}. Determine new $E_{i+1} = E_i - f(E_i)$, μ_{i+1} and ϕ_{i+1}; go to 2.
5. If the total energy is higher than the energy resolution, keep data. If $i < N_{events}$, go to 1.

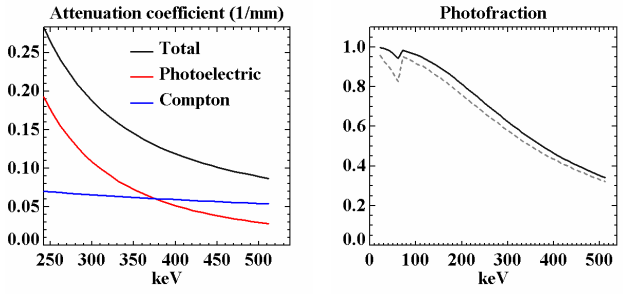

Figure 1. Left: Attenuation coefficient and photofraction for LSO. Right: Photofraction, total and without coherent scatter (dotted line).

The density of the detected energy distribution is obtained for an incident direction ϕ_0. The incident energy E_o is constant (511 keV) and the direction is discretized in spherical coordinates as function of azimutal angle in the detector plane $\varphi, 0 \le \varphi < 2\pi$ and polar angle $\theta, 0 \le \theta < \theta_{\max}$. Where $\theta_{\max}$ is the maximum angle between a LOR and the line normal to the detector plane.

In order to obtain the pixelated crystal iteration probabilities, density distributions $d(\varphi_i, \theta_j)$ are integrated over pixelated crystal volumes. The probabilities depend on the relative position of the incident crystal (Figure 2).

To speed up the process, only the crystals assigned with the M highest probability values are stored in the LUT. A discretization of 1 degree in φ and θ, 256 positions in the pixelated crystal surface, and $M = 16$ (using floating point values) results in 30 million values in the LUT.

C. Scatter simulation

The differential cross section of Compton scattering is given by the Klein-Nishina formula [7]:

$$\frac{d\sigma}{d\varepsilon}=\frac{6\pi r_0^2}{\varepsilon}\left[\left(1-\frac{4}{\varepsilon}-\frac{8}{\varepsilon^2}\right)\ln(1+\varepsilon)+\frac{1}{2}+\frac{8}{\varepsilon}-\frac{8}{2(1+\varepsilon)^2}\right] \quad (3)$$

where r_0 is the classical electron radius and $\varepsilon = 2E/m_e c^2$, being E the energy of incident photon; m_e the electron rest mass and c the speed of light in the air. The energy E' of scattered photons is given by the ratio: $r = E/E' = 1+\varepsilon(1-\cos\psi)/2$; where ψ is the angle between incident and the scattered photon. The energy distribution of scattered photons is determined by the expression:

$$f(r)=\frac{2\pi r_0^2}{\varepsilon\sigma(\varepsilon)}\left[\left(\frac{\varepsilon+2-2r}{\varepsilon r}\right)^2+\frac{1}{r}-\frac{1}{r^2}+\frac{1}{r^3}\right] \quad (4)$$

if $1 \le r \le \varepsilon+1$, and $f(r)=0$ otherwise.
This distribution is sampled by the following technique [7]:

1. Generate 3 random numbers ν_1,ν_2,ν_3 with and uniform distribution in the interval $(0,1)$
2. If $\nu_1 \le 27/(2\varepsilon+29)$, let $r=(\varepsilon+1)/(\varepsilon\nu_2+1)$.
   If $\nu_3 > ((\varepsilon+2-2r)/\varepsilon)^2+1)/2$, go to 1, else accept r.
   Else let $r=\varepsilon\nu_2+1$
   If $\nu_3 > 6.75(r-1)^2/r^3$, go to 1, else accept r.

This algorithm avoids square roots, trigonometric and logarithmic functions, and is optimized for high photon energies. The secondary scattered events with energies below 200 keV are simulated with this alternative algorithm [9]:

1. Generate 3 random numbers ν_1,ν_2,ν_3 with uniform distribution on the interval $(0,1)$
2. If $\nu_1 > (1+\varepsilon)/(9+\varepsilon)$, let $r=(\varepsilon+1)/(\varepsilon\nu_2+1)$.
   If $\nu_3 > ((\varepsilon+2-2r)/\varepsilon)^2+1/r)/2$, go to 1, else accept r.
   Else let $r=\varepsilon\nu_2+1$
   If $\nu_3 > 4(1-1/r)/r$, go to 1, else accept r.

The number of allowed scatters, as well as the minimum energy, can be limited to speed up the process.

D. Transition matrix storage.

A 3D data set (direct and oblique sinograms) is calculated for each voxel and stored in sparse matrix format, since most of the probabilities are zero or have negligible values [10].

The sparseness can be achieved with the limitation of the non-collinearity, positron range, small voxel size or small number of pixelated crystals, but there is a high number of nearly zero probabilities, which are rejected by normalizing and rounding to integer format (16 unsigned bits). Data is divided and ordered in subsets according to the angular dimension. The reconstruction speed depends critically on the number of subsets and rejections.

2-fold axial symmetry and parallel axial redundancies are calculated during the reconstruction process. This limits the application of the proposed method to PET cameras with axial symmetry, but has the advantage that only the values corresponding to the voxels of one direct slice (central slice) have to be calculated, reducing storage and simulation time by two orders of magnitude.

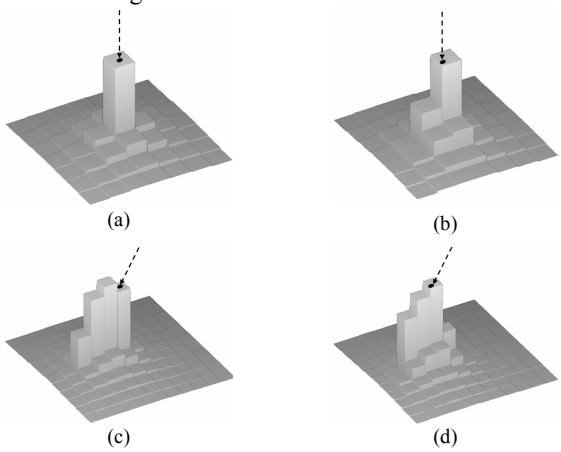

Figure 2. Energy deposition distributions for different incident angles and crystal surface intersection. Values are represented in logarithmic axes normalized to the maximum: (a) $\theta = 0^o$ and entry point in the center of a pixelated crystal. (b) $\theta = 0^o$; entry point not centered. (c) $\theta = 10^o$, centered (d) $\theta = 10^o$, entry point not centered. Crystal maximum probabilities are respectively: 76%, 58%, 37% and 32%.

Additionally, 2D transition matrices can be extracted from the whole 3D data set, using the SSRB algorithm for fast 2D reconstructions.

III. RESULTS

The proposed simulation scheme has been applied to a small animal PET scanner configuration with rotating detector block arrays [11]. This system has four scintillation cameras (Figure 3), composed of 30×35 arrays of 1.5×1.5×12 mm^3 of LYSO ($Lu_{(2-x)}Y_xSiO_5:Ce$) crystals. Tomographic image data are acquired in 3D mode by rotating the gantry in a range of 90 or 180 degrees. Only coincidences between opposed cameras are allowed.

35 direct and 1190 oblique sinograms of 59 radial and 170 angular bins are formed from the collected list-mode data to reach the resolution limit calculated for the scanner and crystal dimensions (Figure 4). The total number of lines of response in this geometry is $35^2 \times 59 \times 170 = 12{,}286{,}750$. The FOV is discretized into $100\times100\times70\times\pi/4 \simeq 5.5\cdot10^5$ voxels, which means that the dimension of the transition matrix **A** is $J \times I \simeq 6.75\cdot10^{12}$ elements. The sparseness and rejection of small values limits to 10^5 the transition matrix elements per voxel. The stored bins for one single slice calculation are $10^5\times100\times100\times\pi/4 \simeq 7.8\cdot10^8$. Using 4 bytes for the position of each matrix element and 2 bytes per element value (in

sparse storage mode), the pre-calculated 3D transition matrix needs less than 5 GB of hard disc space.

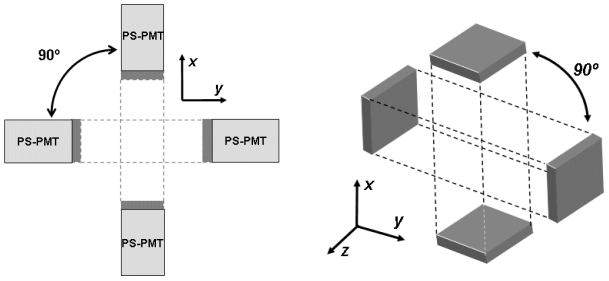

(a) (b)

Figure 3. (a). Scanner geometry, transaxial view, (b) Scanner geometry, 3D model

The 3D-OSEM algorithm only reads a priori probabilities $\mathbf{A} = \{a_{ij}\}$ twice during each EM iteration (projection and back-projection). The lecture is sequential if the subsets are pre-ordered. Using a hard disk with 50 Mbps read velocity the matrix-loading process in each complete 3D-OSEM iteration takes less than 4 minutes. This time is independent on the number of subsets.

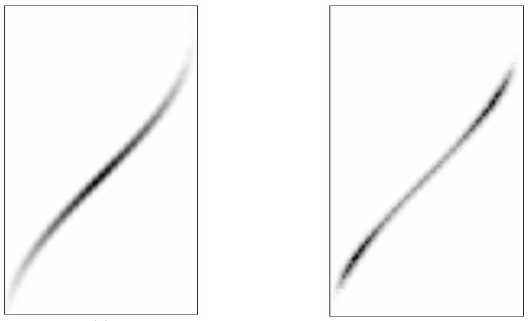

(a) (b)

Figure 4. Visual example of a transition matrix in sinogram mode. Only non-zero elements are stored in sparse mode. (a) Direct sinogram, (b) Oblique sinogram. There are 1225 similar sinograms for a single voxel.

The transition matrix simulation only needs to be calculated once per tomograph configuration. During the design process, however, several geometries are evaluated. The fast simulation method proposed is suitable for the calculation of statistically significant probabilities with 5 seconds of simulation time per voxel, resulting in a total simulation time of approximately 10 hours in a Pentium IV (2.5 GHz) platform. The previously stored crystal LUT takes also a few seconds for each angular discretization.

The exact simulation times depend on many parameters that can be adjusted by the user, like the number of crystals involved (*N* most probable), scatter simulation, voxel size, etc.

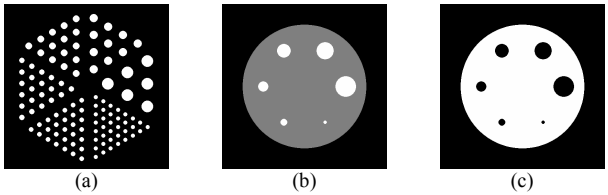

(a) (b) (c)

Figure 5. Phantoms simulated with SimSET: (a) Derenzo-type phantom. Rods diameters (mm): [3.4, 2.4, 2.0, 1.6, 1.4, 1.2]. Total coincidences (70 slices): $10.3 \cdot 10^6$, (b) Rods activity density two times the background activity, rods (mm): [6.0, 5.0, 4.0, 3.0, 2.0, 1.0], Total coinc. (70 slices): $24 \cdot 10^6$(c) Rods (mm): [6.0, 5.0, 4.0, 3.0, 2.0, 1.0] Total coinc. (70 slices): $20.5 \cdot 10^6$

We have used SimSET [12] to generate realistic data sets of phantom activity distributions for the scanner configuration described above (Figure 5), in order to validate the methodology proposed. Preliminary reconstructions have been made with the system matrix calculated as described here. The 3D-OSEM reconstruction in the central transaxial plane is shown (100x100 pixels, slice 34 of 70), as well as a SSRB+FBP with axial rebinning of 5 crystals and Hanning window smoothing (128x128 pixels, slice 34 of 69). 3D-OSEM has been performed with 10 subsets and 5 iterations, without Bayesian regularization, scatter and attenuation correction (Figure 6).

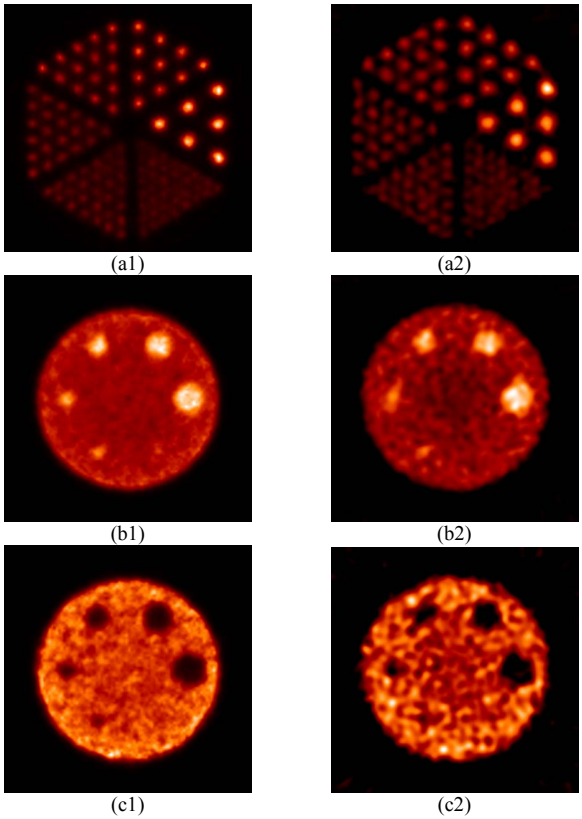

(a1) (a2)

(b1) (b2)

(c1) (c2)

Figure 6. Reconstructions of phantoms in Figure 5. (a1,b1,c1) 3D-OSEM reconstructions, 5 iterations, 10 subsets. (a2,b2,c2) SSRB-5 + FBP (Hanning window)

IV. Conclusions

An efficient method for the calculation of the transition matrix for 3D iterative image reconstruction based on Monte Carlo techniques has been presented. The model (adapted to a high resolution PET system for laboratory animal imaging) incorporates not only the geometrical configuration of the tomograph, but also detailed a-priori information on the physical process of the γ-event detection by the scintillation crystals. Future work will include incorporation of further models corresponding to the response of the photomultiplier tubes and the front-end electronics of the system. The inclusion of phoswich crystals for depth-of-interaction (DOI) computation is also straightforward.

V. Acknowledgements

This work has been partly funded by the Spanish Ministry of Science & Technology (TIC 2001-0175-C03) and by the Spanish Ministry of Health (Red Temática IM3, G03/185).

The authors wish to thank José Luis Contreras from Univ. Complutense de Madrid, and Juan J. Vaquero and Manuel Desco, from the G.U Gregorio Marañón Hospital (Madrid, Spain) for motivation discussions and fruitful comments.

VI. References

[1] L.A. Shepp and Y. Vardi, "Maximum Likelihood Reconstruction in PET", IEEE Trans. Med. Imag., 1:113-122, 1982.

[2] H.M Hudson, and R.S Larkin, "Accelerated Image Reconstruction Using Ordered Subsets of Projection Data". IEEE Trans. Med. Imag, 13(4): 601-609, 1994.

[3] G. Kontaxakis, L.G. Strauss and G.S. Tzanakos, "An Efficient Implementation of the Iterative ML-EM Image Reconstruction Algorithm for PET on a Pentium PC Platform", J. Comp. Inf. Tech., 7(2): 153-163, 1999.

[4] M. Defrise, P.E Kinahan, D.W Townsend, C. Michel, M. Sibomana and D.F. Newport. "Exact and Approximate Rebinning Algorithms for 3D-PET Data". IEEE Trans. Med. Imag., 16:145-158; 1997.

[5] S.F. Haber, S.E. Derenzo and D. Huber, "Application of mathematical removal of positron range blurring in positron emission tomography", IEEE Trans. Nucl. Sci, 37(3):1293:1299, 1990.

[6] C.A Johnson, Yuchen Yan, R.E Carson, R.L Martino, M.E Daube-Witherspoon, "A system for the 3D reconstruction of retracted-septa PET data using the EM algorithm", IEEE Trans. Nucl. Science, 42(4): 1225-1227, 1995.

[7] Hua, X. "Monte Carlo Simulation of Comptonization in Inhomogeneous Media", Computers in Physics, 11(6):660-668, 1997.

[8] M.J Berger, J.H Hubbell, S.M Seltzer, J.S Coursey and D.S Zucker, "XCOM: Photon Cross Sections Database", NIST Standard Ref. Database: http://physics.nist.gov/PhysRefData/Xcom/Text/XCOM.html

[9] A.J. Ball, "Measuring Physical Properties at the Surface of a Comet Nucleus", Ph.D. Thesis. University of Kent, Canterbury, UK,1998.

[10] J.E Ortuño, J.J Vaquero, G. Kontaxakis, M. Desco, A. Santos. "Preliminary Studies on the Design and Simulation of High Resolution Small Animal PET Scanners with Octagonal Geometry", IEEE Med. Imag. Conf. (MIC), Portland, 2003.

[11] J.J. Vaquero, A. Molins, J.E. Ortuño, J. Pascau, M. Desco, "Preliminary Results of the Small Animal Rotational Positron Emission Tomography Scanner," Mol. Imag. Biol., 6(2):102, 2004.

[12] SimSET homepage: http://depts.washington.edu/~simset/html/